An Automatic Fingerprint Classification Technique based on Global Features

Saparudin and Ghazali Sulong

Abstract— **Fingerprint classification is an important stage in automatic fingerprint identification system (AFIS) because it significantly reduces the processing time to search and retrieve in a large-scale fingerprint database. However, its performance is heavily relied on image quality that comes in various forms such as low contrast, wet, dry, bruise, cuts, stains, etc. This paper proposed an automatic fingerprint classification scheme based on singular points and structural shape of orientation fields. It involves several steps, amongst others: firstly, fingerprint foreground is extracted and then noise patches in the foreground are detected and enhanced. Next, the orientation fields are estimated, and a corrective procedure is performed on the false ones. Afterward, an orientation image is created and singular points are detected. Based on the number of core and delta and their locations, an exclusive membership of the fingerprint can be discovered. Should it fail, the structural shape of the orientation fields neighboring the core or delta is analyzed. The performance of the proposed method is tested using 27,000 fingerprints of NIST Special Database 14. The results obtained are very encouraging with an accuracy rate of 89.31% that markedly outperformed the latest work.**

Index Terms—**fingerprint classification, orientation fields, singular points, structure shape.**

I. Introduction

FINGERPRINT identification needs to search the entire database to find the potential corresponding ones to the query fingerprint. The huge amount of data from the large fingerprint databases compromises the efficiency of the identification task, although the fastest matching algorithms take only a few milliseconds per matching. To perform fingerprint identification, both matching accuracy and processing time are critical performance issues. In order to achieve an efficient identification, fingerprints in the database are organized into a number of mutually exclusive classes that share certain similar properties. This process is called fingerprint classification. Therefore, although all automatic fingerprint identification systems require the fingerprint classification stage before the matching stage, it is very difficult to design an automatic system able to perform such classification with high accuracy [1].

Most modern fingerprint classification is using five classes, namely; Arch, Tented-arch, Left-loop, Right-loop, and Whorl. The distribution of the classes in nature is not uniform. The probabilities of the classes are approximately 0.037, 0.029, 0.338, 0.317, and 0.279 for the Arch, Tented-arch, Left-loop, Right-loop, and Whorl, respectively [3]. Left-loop, Right-loop and Whorl are the most common, making up 93.4% of all fingerprints.

Therefore, for developing and testing of a classification system, it is important to use a suitable dataset with sufficient sample size that can represent the natural distribution of human fingerprints' classes. However, most researchers employed NIST Db-4 and insufficient samples (i.e. Less than 10,000 prints) for testing and validating their experiments [1], [5], [6], [7], [8], [9]. Sasikala and Prabha [10] employed 880 fingerprints in FVC2000 database for evaluating fingerprint classification. Thus, their experimental results' validity is disputable, and consequently the performance of their proposed classification methods is also implausible [11]. In relation to that, NIST Special Database 14 (NIST Db-14) was created and becomes de facto standard data set for developing and testing of automatic fingerprint classification systems [11], [12].

Naturally, there are some fingerprints that are ambiguous and cannot be classified even by a human expert because in some cases, the fingerprints have properties more than one class. In these cases it is unclear which fingerprint classes the ambiguous prints should be matched against.

Fingerprint images of poor quality due to scars and injuries are often difficult to classify, even for a human expert: in many applications such images are rejected. Because this would be less damaging than a wrong decision. For this reason, to improve the accuracy, several classification approaches apply a rejection mechanism in which the images are classified as "unknown".

There is always a possibility of misclassification due to noise, especially generated by excessive or insufficiently used by ink during the fingerprint imprinting process. In relation to that, there are many dry, wet and bruises prints existed in the NIST Db-14 which is considered to be unfavorable quality. The database also contains images that are often tainted by handwritten annotations and other artefacts common for inked-fingerprints. Generally, manually cropping of fingerprint images is a commonly used pre-processing in order to remove the annotations and artifacts [13]. Besides, cropping and alignment are also manually applied for extracting and realignment of a foreground image. A foreground of size 500×500 pixels and in the upright position is more preferable as a work area by most researchers. However, the above processes are considered non-automatic or semi-automatic because of human intervention, and should be avoided if possible. Therefore, developing a full-scale automatic fingerprint

Manuscript received November 21, 2015; revised February 17, 2016.

Saparudin is with the Department of Informatics Engineering, Universitas Sriwijaya, Palembang, Indonesia (e-mail: saparudin1204@yahoo.com).

Ghazali Sulong is with the Department of Software Engineering, Universiti Teknologi Malaysia, Johor Bahru, Malaysia (e-mail: ghazali@utmspace.edu.my).

(Advance online publication: 27 August 2016)

classification system is considered to be a very challenging task.

The majority of classification is a large distinction among orientation patterns of ridge structure within the same class, especially in the whole case. This problem is usually termed as large-intra-class variation, in which the prints of the same class have distinct characteristics causing the similarity measure having to cover large spread, and therefore is difficult to classify [14]. Moreover, in some cases, prints from one class can appear very similar to prints from another class, particularly arch and arch-like classes (i.e. Left-loop, Tented-arch and Arch). In other words, there is a small-inter-class variation. This interclass problem is extremely difficult to deal with even for a human expert.

Choosing the distinguishable features is very important for the fingerprint classification which can affect its performance. The category of a fingerprint is determined by its global ridges and valleys structures. There are two kinds of features for its representation: global features that describe the flow structure of ridges and local features that describe the minute details of ridges. The classification of a fingerprint is based on its global pattern of ridges and valleys. A valid feature set for fingerprint classification should be able to capture this global information effectively [15]. Therefore, it is natural to base the features directly on the fingerprint ridges. There are many different ways to extract and represent ridge information. Orientations fields are convenient to summarize the ridge-valley patterns of a fingerprint. Fingerprint ridge orientation estimation, especially for low quality image, is still a challenging problem in automatic fingerprint classification and new creative methods for orientation estimation and correction are expected to be proposed and investigated [16].

There is a wide variety of orientation fields-based classification methods that have been proposed by previous researches, including geometric-based, structure-based, rule-based, learning-based, statistically-based, and hybrid [11], [15]. However, most of the techniques are considered rigid and involving human intervention during a pre-processing stage. Moreover, most of their experiments were based on unreliable dataset such as NIST Db-4 which contains 2000 pre-segmented and pre-cropped prints [13]. This limited number of pre-processed prints is considered to be small and unnatural, and therefore, is not reliable to be an appropriate testing platform for the fingerprint classification. In addition, some studies have also employed standard dataset but with unreliable sample size (i.e. Insufficient and biased), except for Cappelli and Maltoni [13]. Therefore, the results of their experiments and as well as the proposed method are disputable.

Another feature that is often used for distinguishing fingerprint classes is the existence and location of singular points. The singular points are classified into core and delta. The difficulties faced by singularities-based are as follows: The singular points may not appear in the image, especially if the image is small; the noise in the fingerprint images makes the singular point extraction unreliable, including missing or wrong detection. Several methods have been proposed to locate the singular points. However, the most common and widely used is the Poincare index [14], but this method is very sensitive to noise, low contrast and quality of fingerprint images.

Local averaging of the orientation fields are often quite effective in preventing the detection of false singular points, even if it can lead to slight displacement of the delta position toward the borders [11]. Park *et al.* [17] proposed the orientation of any two horizontally adjacent elements is checked against a set of pre-defined rules to detect candidate regions of singular points; for each candidate region, its neighboring elements are then analyzed to confirm the presence of singular points. This method is very sensitive to fingerprint image rotation because only the upper and lower cores are used. Wang and Xie [8] employ structure shape of orientation fields around the cores when the delta located near the border are failed to be detected.

In relation to that, many techniques have been proposed to locate the singular points; their performances are far from satisfactory, let alone a full automation. Therefore, it is vital to come out with an efficient technique that is capable of detecting precisely genuine singular points without undergoing both cropping and realignment pre-processes.

This paper presents a new automatic fingerprint classification technique based on singular points and structural shape of orientation fields. The process involved five main parts, namely; segmentation, enhancement, orientation field estimation, singular points detection, and classification. The rest of the paper is organized into sections. Section 2 is the related work of the study, which is followed by methodology in section 3, while the results of the experiments are explained in detail in section 4. The summary and concluding remarks are given in section 5.

II. Related Work

Fingerprint classification refers to the problem of assigning a fingerprint to a class in a consistent and reliable way. Fingerprint classification is generally based on global features, such as global ridge structure and singularities [10]. The ridge structure characterizes the shape described by the ridge flows. The singularities or singular points are localized in small areas where the ridge flow becomes irregular. The most of the classification schemes used are currently based on the Galton-Henry classification scheme. They have introduced the concept of singularities in the fingerprint classification. According to the number and position of the singular point, a fingerprint can be classified into classes. The five most common classes are:

1. Arch; ridges enters from one side, rise gradually and bulge to form a small bump, and exit on the opposite side. It does not contain any core or delta.
2. Tented-arch; similar to the arch except that at least one ridge has a high curvature that resembles like a peak. This class has one core and one delta points whose locations are vertically aligned with respect to each other.
3. Left-loop; one or more ridges enter from the left side, curve back, and go out the same side as they entered. One core and one delta are present.
4. Right-loop; same as the left loop, but the direction of ridges entrance and exit is from the right side. One core and one delta are present.

5. Whorl; contains at least one ridge that makes a complete 360-degree path around the center of the fingerprint. Two cores and two deltas are found.

Fingerprint classification is considered as a difficult pattern recognition due to the small- inter-class variability, the large-intra-class variability, ambiguous prints, and poor quality fingerprint image, which makes the classification task even more difficult. Several approaches have been developed for automatic fingerprint classification. These approaches can be broadly categorized into four main categories: *rule-based*, *structure-based*, *frequency-based*, and *syntactic* [15]. Maltoni *et al.* [11] added three more categories: *statistical, neural network-based, and multi-classifier*. In this paper, rule-based and structure-based approaches will be explored in great details as they are related to methodology used in this research.

A. Rule-Based Approaches

The heuristic rule-based fingerprint classification technique, and sometimes is also called model-based approach, uses the number and the locations of singular points to classify a fingerprint. This approach was first introduced by Henry [18] in his manual classification in the early 1990s. Later, the idea is adopted by Karu and Jain [1] to automatically classify the fingerprints. Their approach consists of three major steps: (i) computation of the ridge directions using 9×9 mask, (ii) finding the singularities in the directional image using Poincare index, and (iii) classification of the fingerprint based on the detected number and location of singular points. The classifier was tested on 4,000 and 5,400 images in the NIST-Db-4 and DB9, respectively. For both databases, classification accuracies of 85.4% for the five - class and 91.1% for the four-class problems, respectively, are reported. Since the method solely relies on the singular points, failure to locate them will result in classification errors. In other words, the method is only suitable for good quality fingerprints. Due to the limitations mentioned above, most of the recent studies combine singularities with another feature, such as ridge orientation field [11].

Chong *et al.* [19] proposed rule-based approaches without singular point. The classification of five classes is based on the geometric framework. The framework employs both a geometric grouping and a global geometric shape analysis of fingerprint ridges. Unfortunately, the real performance of the method could not be verified since tested sample is very small (i.e. Less than 100 prints) and therefore is considered unreliable.

Hong and Jain [5] have combined the orientation field information with available ridge details of fingerprint classification. However, their method does not reliably handle poor quality fingerprints when the orientation field is very noisy and it can be misled by poor structural cues in the presence of finger cuts and faults on the skin. Zhang and Yang [7] and Wang and Dai [9] use both singularities and a pseudo-ridge tracing algorithm to classify the fingerprint when only one singular point (a loop or a delta) is found. This method has been tested on 4,000 images in NIST-DB 4 database. Classification accuracy reaches 92.7% for the four-class problem.

A further problem with the singular point based approaches is that, it may not work well on inked based fingerprint because deltas are often missing in these types of images. In relation to that, Cho *et al.* [20] proposed a method that uses only the cores and classifies fingerprints according to the curvature and orientation fields surrounding the core. Jain and Minut [6] proposed rule-based approaches that do not search for any singularity: the classification is based on the geometrical shape of the ridge lines. For each class, a fingerprint kernel which models the structural shape of fingerprints in that class is defined; the classification is then performed by finding the kernel that best fits the orientation image of the given fingerprint. Moreover, Wang and Xie [8] combined singular points and analysis of fingerprint structures in fingerprint classification. Image orientation is divided into non-overlapping partitions to give a synthetic representation. Singular points are extracted using Poincare index. The method is invariant to rotation, translation and small amounts of scale changes. Later, Li *et al.* [21] combined interactive validation algorithm of singular points and constrained non-linear phase portrait orientation-field model for fingerprint classification. The combined orientation and singularity features are used to classify fingerprints using an SVM classifier.

Tan *et al.* [22] proposed a fingerprint classification method based on analysis of singularities and geometric framework. Firstly, a pseudo-ridges extraction algorithm is applied to extract the global geometric shape of fingerprint ridges of pattern area. Then, by using the detected singularities coupled with global shape analysis of orientation fields, the fingerprint is classified. This algorithm has been tested on 1,000 images of NJU database, which contains 2,500 fingerprints. The classification accuracies are 87% for five-class problems. Unfortunately, this self-created database is hardly known and unreliable.

Cappelli and Maltoni [13] proposed the spatial distributions of singularity locations in nature and derive from the probability density functions of the four fingerprint classes. The results obtained can be directly exploited to improve the accuracy of fingerprint classification. Firstly, each fingerprint image in NIST Db-14 is cropped using the approach proposed in [23]. Secondly, the fingerprint is segmented using the approach proposed in [24]. Thirdly, the orientation fields are estimated with a gradient-based technique proposed in [25]. Fourthly, the iterative singularity detection approach proposed in [1] is adopted to find the number and the positions of the singular points. Finally, for each class, an estimation of the probability density function of singularity locations is obtained as a mixture of Gaussians. The proposed method has been tested on 27,000 fingerprint images of NIST Db-14. The classification accuracy of 81.2% for five-class problem is reported.

The Pseudo-singularity-points for classifying the fingerprints is proposed in [26]. This method is based on singular points and regions of orientation fields adjacent to the singular points. Firstly, singular points are detected using Poincare index, and finally, false singular points are analysed using Pseudo-singularity-points. This method has been tested on 1,024 fingerprint images, which consist of 80, 80, 800, and 80 fingerprint images of databases FVC2000 DB1-B, FVC2002 DB2-B, FVC2002 DB2-A and NIST DB4, respectively. They claimed 12.25% error rate of fingerprint classification.

B. Structure-Based Approaches

The orientation image is well suited for structural representation of fingerprint images. Generally, the image is first partitioned into several distinct regions of homogenous orientation fields. This approach is adopted by many researchers, including [2], [27].

In [27], it consists of five steps: orientation image formation; orientation image partitioning according to the respective homogenous regions using a dynamic clustering algorithm; construction of the relational graph according to the homogenous regions; graph matching; and classification. The classification is carried out using template matching of the graphs.

However, their study yields no conclusive result that can be used to measure the performance of their approach. Later, Cappelli *et al.* [2] have improved the Maio and Maltoni's [27] work by using dynamic masks to produce a numerical vector representing each fingerprint as a multidimensional point, which can be conceived as a continuous classification.

Meanwhile, Cappelli *et al.* [28] coupled the dynamic mask approach (MASKS) and the Multi-space KL (karhunen-loeve) transform' to classify fingerprint image. Due to the high variability of the homogeneous regions, it is difficult to find a set of graphical prototypes that can be used as a template. Furthermore, in actual fact, template matching of the graph-prototypes is ineffective to discriminate between fingerprint classes, especially involving small-inter-class variation.

In [29], the problem of finding an effective set of graph-prototypes have been addressed. They proposed a new approach to form the homogeneous region using the variance of orientation fields. They claimed that number of graph-prototypes are markedly reduced. Their experiment utilizing 4,000 fingerprints of NIST Db-4 has revealed that 60 prototypes have been obtained, and 80.25% accuracy is achieved, which outperformed other graph-matching based approaches.

Wang and Xie [8] used analysis of the fingerprint structure to classify fingerprint images. Flow-like tracing technique is used to analyse the fingerprint structures. By tracing from the inner side to the outside of a core, they can see that there is a tendency of angle variation. Their algorithm paid special attention on single core cases whose exclusive class cannot be established. It is performed by tracing the orientation fields in two opposite directions, namely leftward and rightward, and starting from the core point. By doing so, the class of the fingerprint can be established, which is either Left-loop, Right-loop or Tented-Arch.

III. Proposed Method

In this paper, a new scheme of fingerprint classification is proposed based on ridge structure and singular points. With regard to this, there are eight processes involved that link with the generic scheme, which include: foreground extraction, identification and marking of noise area, noise removal, orientation field estimation, refinement of orientation fields in the noisy areas, determine the candidate region of the singular point, identification of core and delta, and classification. The following paragraph brief presents step-by-step of the proposed scheme.

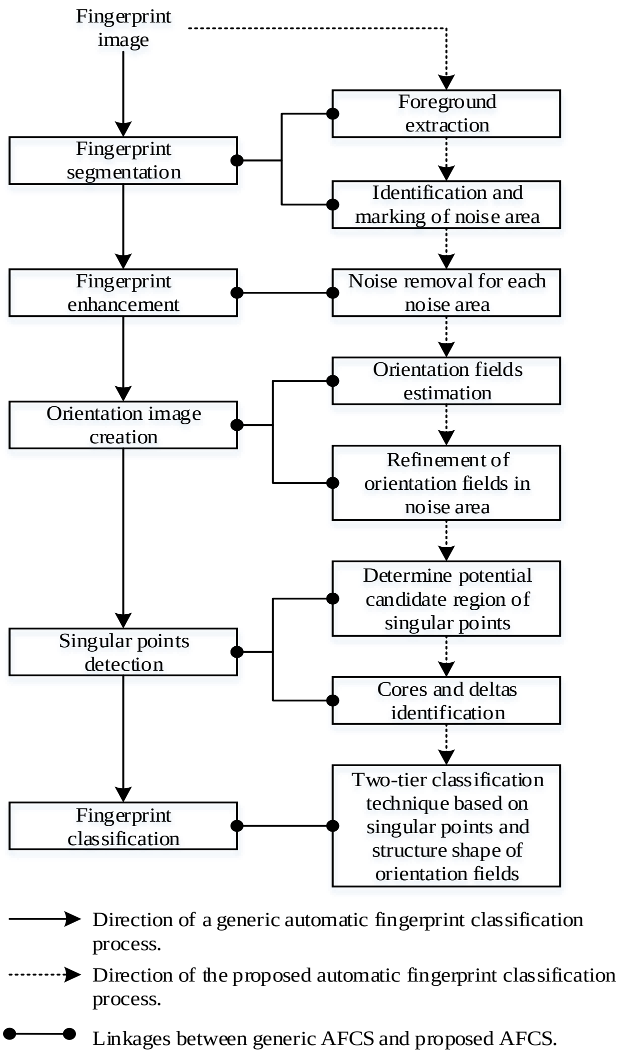

Fig. 1 On Automatic Fingerprint Classification Scheme (AFCS): Proposed AFCS complements generic AFCS (Note: The dashed rectangle denotes the proposed AFCS).

Firstly, a fingerprint image is partitioned into 16×16 blocks of pixels. Immediately after that, a foreground is separated from the image using block-wise operations in which a composite method, which combines local mean values of the grey-levels with local variances of the gradient magnitudes, is implemented. Secondly, noise regions in the foreground are detected using coherence values of ridges' gradients, and then are enhanced using the minimum variance of gradient magnitude. Thirdly, for each marked noise region, its noises are removed. Fourthly, Least Mean Square orientation field estimation algorithm is then applied to estimate the orientation fields of each block, and finally an orientation image is created once all orientation fields are computed. Normally, the resultant orientation image contains some false orientation fields due to various reasons, and this drawback is resolved by using the minimum variance of the orientation fields approach, and this is considered as fifth stage. Next, the orientation image is partitioned into several distinct regions whose memberships are characterised by homogenous orientation fields. The convergence point of these regions implicitly reveals a potential candidate of the singular point region and this is considered sixth stage. Subsequently, the famous Poincare index is applied to each singular point region to determine core and delta. The first step up to seventh adopted in [4].

Now, with this invaluable information equipped with the number of core and delta and their locations, an exclusive membership of the fingerprint class can be determined. Should the classification could not be ascertained, then the structure shape of the orientation fields surrounding the singular point is examined. This classification approach hereinafter named two-tier classification technique is proposed and an in depth discussion is provided in this paper. The entire classification scheme is depicted in Fig. 1.

Various classifiers have been proposed by previous studies to classify the fingerprint into one of the pre-specified types that include: Ruled based, Sequential, Majority vote rule, neural network and k-nearest neighbour. Yet, their performances are still far from satisfactory. This motivates to propose a new rule-based strategy that combines singular point based method and structure shape of orientation fields, and named as *Two-tier fingerprint classification technique*.

Generally, this technique involves two main phases: First, the core and delta obtained from singular point detection using Poincare index are further analysed in terms of their counts and locations. If the numbers of core and delta satisfy the pre-defined rules then the fingerprint is assigned to a specific class. Otherwise, proceed to the second phase in which the structure shapes of the orientation fields surrounding the core or delta are examined in depth. If the characteristics of the shapes meet the pre-defined rules then the fingerprint is allocated to a specific class. This sequential process is called two-tier classification.

A. *The Classification Rule*

Once the cores and deltas have been determined in terms of their numbers and locations, next is to decide to which class the fingerprint belongs. The classification rules are as follows:

1. Let Nc and Nd be number of cores and deltas, respectively.
2. If $Nc = 0$ and $Nd = 0$, then an Arch is assigned to the fingerprint image.
3. If $Nc = 1$ and $Nd = 1$, then check the position of the delta with respects to the core:
   a. Let (x_c, y_c) and (x_d, y_d) be the position of core and delta, respectively.
   b. If the delta is on the right of the core, which is, $x_c - x_d <= -16$, then a Left-loop class is assigned to fingerprint.
   c. If delta is on the left of the core, that is, $x_d - x_c >= 16$, a Right-loop is assigned.
   d. If delta is below core, which means, $x_c - x_d > -16$ and $x_c - x_d < 16$, a Tented-arch is allotted.
4. If $Nc = 2$ and $Nd = 2$, a Whorl is assigned;
5. $Nc > 1$, means that there is a possibility that some of the detected cores are fake. Therefore, the cores are further analysed to determine their authenticity, and to accomplish that, the structural shapes of orientation fields that neighbouring each core are investigated using technique of section 3.2 below. Once the process is completed, step 2 to step 4 are then repeated.
6. $Nd > 1$, reflects that some false deltas are existed, and thus an in depth analysis of the orientation fields surrounding the deltas is required. With regards to that, technique of section 3.2 below is proposed to eliminate the fake deltas. Once the process is done, step 2 to step 4 are resumed.
7. If $Nc = 1$ and $Nd = 0$, it means that there is a possibility that a delta may exist but could not be detected previously. Normally, this is due the fact that the delta is located close to the boundary of the foreground. Thus, an in depth analysis is required to determine its existence by examining orientation fields neighbouring the core. This structural shape analysis is given in sub-section examine true cores below.
8. If $Nc = 0$ and $Nd = 1$, it means that this conjecture complements to the above case signifies that a core may exist, but failed to detect by the Poincare index. In actual fact, this is rarely seen in this study, and it may happen due to noises that are still remaining and located close to the core. Hence, a detailed analysis of the orientation fields' patterns surrounding the delta is provided – a thorough discussion is given in sub-section examine true deltas below.
9. Otherwise, reject the fingerprint image.

B. *Structure Shape Analysis of Orientation Fields*

There are four situations that require further analysis of the orientation fields that neighbouring the core or delta, which are: (1) Number of cores is more than one, (2) Number of deltas is more than one, (3) Number of core is one and delta is zero, and (4) Number of delta is one and core is zero. These cases certainly require in depth analyses and therefore are provided in the following sub-sections.

Examine True Cores

The algorithm for deciding true core points is divided into two stages. Firstly, examine the structure shapes of three-neighbourhood orientation fields surrounding the core. There are four possible core shapes characterized by neighbouring orientation fields namely, upper-core, lower-core, right-core and left-core as depicted by Fig. 2 below. Secondly, examine the structure shapes of twenty four orientation fields neighbouring the core as depicted by Fig. 3 below.

Detailed description of the first stage is performed as follows:

1. Let's define angles of a core point and its three-

directional neighbours (i.e. right-side, lower-side, and lower-right-side) as $\theta'''(i_c, j_c)$, $\theta'''(i_c+16, j_c)$, $\theta'''(i_c, j_c+16)$, and $\theta'''(i_c+16, j_c+16)$, respectively.

2. The types of the core using neighbourhood operations are determined. For the upper-core and lower-core: (i) compare the angle of orientation field at core point $\theta'''(i_c, j_c)$ with $\theta'''(i_c+16, j_c)$ and (ii) compare $\theta'''(i_c, j_c+16)$ with $\theta'''(i_c+16, j_c+16)$. Details are given below:
   a. Upper-core:
      If {($0^o \le \theta'''(i_c, j_c) < 90^o$ and $90^o \le \theta'''(i_c+16, j_c) \le 180^o$) or ($0^o \le \theta'''(i_c, j_c+16) < 90^o$ and $90^o \le \theta'''(i_c+16, j_c+16) \le 180^o$)}, then the type is upper-core.
   b. Lower-core:
      If {($90^o \le \theta'''(i_c, j_c) \le 180^o$ and $0^o \le \theta'''(i_c+16, j_c) < 90^o$) or ($90^o \le \theta'''(i_c, j_c+16) \le 180^o$ and $0^o \le \theta'''(i_c+16, j_c+16) < 90^o$)}, then the type is lower-core.
3. Meanwhile, for the right-core and left-core: (i) compare the angle of core point $\theta'''(i_c, j_c)$ with $\theta'''(i_c, j_c+16)$ and (ii) compare the angle of its right-side neighbour $\theta'''(i_c+16, j_c)$ with $\theta'''(i_c+16, j_c+16)$. Details are as follows:
   a. Right core:
      If {($90^o \le \theta'''(i_c, j_c) \le 180^o$ and $0^o \le \theta'''(i_c, j_c+16) < 90^o$) or ($90^o \le \theta'''(i_c+16, j_c) \le 180^o$ and $0^o \le \theta'''(i_c+16, j_c+16) < 90^o$)}, then the type is right-core.
   b. Left core:
      If {($0^o \le \theta'''(i_c, j_c) < 90^o$ and $90^o \le \theta'''(i_c, j_c+16) \le 180^o$) or ($0^o \le \theta'''(i_c+16, j_c) < 90^o$ and $90^o \le \theta'''(i_c+16, j_c+16) \le 180^o$)}, then the type is left-core.

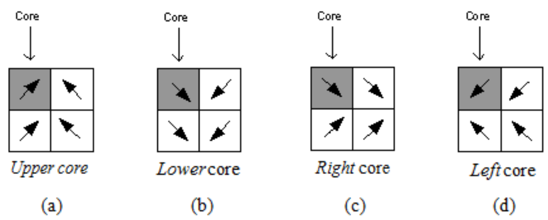

Fig. 2 Types of the core point (a) Upper-core, (b) Lower-core, (c) Right-core, and (d) Left-core.

Once the type of the core is found, then the second stage is resumed, otherwise proceed with the search for the next core. The second stage is performed as follows:

1. Define four-directional groups of orientation fields (or GOF in short) that adjacent to the core as GOF-left, GOF-right, GOF-top and GOF-bottom. In upper-core and lower-core cases: the GOF-left and GOF-right consist of twenty four orientation fields neighbouring the core that organized in eight rows and three columns, and situated on the left and right sides of the core, respectively (see Fig. 2 (a) and (b)). Meanwhile, for the right-core and left-core: the groups are represented by GOF-top and GOF-bottom with block size of 3×8 orientation fields (see Fig. 2 (c) and (d)).
2. With regard to that, let all the symbols used to represent number of orientation fields associated with the GOFs be defined as follows: (i) $Nr[90]$ and $Nr[180]$ denote the numbers of orientation fields of GOF-right whose angles are in the ranges of $0^o \le \theta'''(i,j) < 90^o$ and $90^o \le \theta'''(i,j) \le 180^o$, respectively. (ii) $Nl[90]$ and $Nl[180]$ denote the numbers of orientation fields of GOF-left whose angles are $0^o \le \theta'''(i,j) < 90^o$ and $90^o \le \theta'''(i,j) \le 180^o$ ranges, respectively. (iii) $Nt[90]$ and $Nt[180]$ denote the numbers of orientation fields of GOF-top whose angles are in the ranges of $0^o \le \theta'''(i,j) < 90^o$ and $90^o \le \theta'''(i,j) \le 180^o$, respectively. (iv) $Nb[90]$ and $Nb[180]$ denote the numbers of orientation fields of GOF-top whose angles are in the ranges of $0^o \le \theta'''(i,j) < 90^o$ and $90^o \le \theta'''(i,j) \le 180^o$, respectively.
3. If ($Nr[180] \ge T3$ and $Nl[90] \ge T3$) then upper-core is true; otherwise, if ($Nr[90] \ge T3$ and $Nl[180] \ge T3$) then lower-core is true. On the other hand, if ($Nt[180] \ge T3$ and $Nb[90] \ge T3$) then right-core is true; otherwise, if ($Nt[90] \ge T3$ and $Nb[180] \ge T3$) then left-core is true. Where $T3$ denotes a threshold value that determine the true core. In this study, the empirical value of $T3$ is 10.

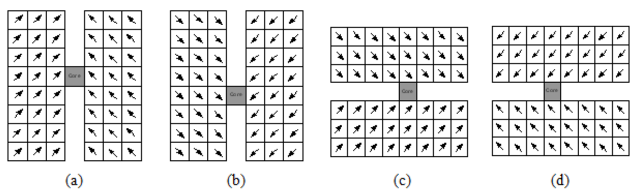

Fig. 3 Omni-directional orientation fields neighbouring the core points: (a) Upper-core, (b) Lower-core, (c) Right-core, and (d) Left- core.

Examine True Deltas

Similarly, the following procedure is proposed to determine the authenticity of the deltas obtained in section III.B above.

Let $\theta'''(i_d, j_d)$ for $d = 2, 3, \ldots, n$ be the angles of orientation field at delta points. Let's define three-directional groups of orientation fields that neighbouring the delta on the left, right and top directions as GOFD-left, GOFD-right and GOFD-top whose dimensions are 4×4, 4×4 and 10×1, respectively (see Fig. 4 (a) and (b)).

1. In addition, define $Nr[90]$ and $Nr[180]$ as the numbers of orientation fields of GOFD-right whose angles are in the ranges of $0^o \leq \theta'''(i_d, j_d) < 90^o$ and $90^o \leq \theta'''(i_d, j_d) \leq 180^o$, respectively. Similarly, let $Nl[90]$ and $Nl[180]$ denote the numbers of orientation fields of GOFD-left whose angles are in the ranges of $0^o \leq \theta'''(i_d, j_d) < 90^o$ and $90^o \leq \theta'''(i_d, j_d) \leq 180^o$, respectively. Also, define Nu as the number of orientation fields of GOFD-top, which has angles in the range of $75^o \leq \theta'''(i_d, j_d) \leq 105^o$.
2. If {($Nr[180] \geq T4$ and $Nl[90] \geq T4$) or $Nu \geq T5$ }, then delta is true. Where $T4$ and $T5$ denote threshold values that determine the true delta. In this study, the empirical values of $T4$ and $T5$ are 6 and 4, respectively.

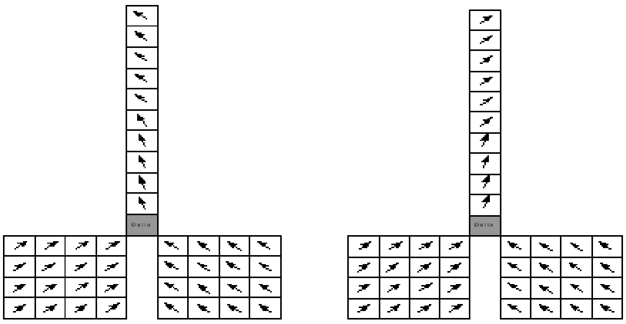

(a) (b)

Fig. 4 Omni-directional orientation fields neighbouring a delta. (a) Right-delta and (b) Left-delta

IV. Experiment Result and Discussion

The experiment has been conducted using 27,000 fingerprint images acquired from NIST Db-14 (i.e. file names: f0000001 – f0027000) to evaluate the performance of the proposed classification technique. The prints are 8-bit greyscale and sized 832 x 768 pixels. Furthermore, there is about 25,880 of the fingerprints were obtained from ink-on-paper rolled impressions. As a result, a lot of associated problems inherently emerged, such as noises, ink stains, translation and rotation due to excessive or insufficient ink on the finger [11], [30].

TABLE I
Classes of fingerprint NIST db-14

Classes	Count	% of total
Whorl	8,330	30.85
Left-loop	8,619	31.92
Right-loop	8,239	30.51
Arch	976	3.61
Tented-arch	815	3.02
Scar	21	0.08
Total	27,000	

Table I shows detailed information about the distribution of classes in the dataset by the human expert, and it reveals that Whorl, Left-loop, and Right-loop combined constitutes exactly 93.29% of the fingerprints, which reflects the natural distribution of the population fingerprint classes.

Furthermore, there are about 6.63% of the total fingerprints in NIST Db-14 is categorised as ambiguous print [13] whose exclusive membership cannot be positively determined by human experts. Normally, this type of print carries multiple patterns of ridge structure that belong to two or more different classes. As a result, it may lead to misclassification. For instance, fingerprint f0000042 as shown in Fig. 5, which is manually labelled as “co/09”, the print is classified as a Whorl, but the right delta is near the core making it similar to the Right-loop so it was given another code which is a “09” reference. In other words, the fingerprint has dual classes i.e. Whorl and Right-loop. Normally, in such a case, as a rule of thumb, the class of the ambiguous print is accepted as a true class if its hypothesized class is matched by either one of the classes. However, in NIST Db-14, the class is already rigidly fixed according to one of the labelled classes, making it more difficult to correctly match with the hypothesized one, which may lead to misclassification mistakenly.

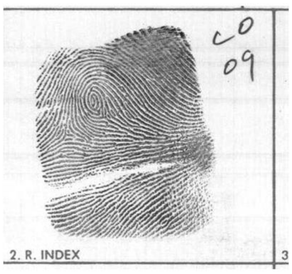

Fig. 5 Fingerprint with a cross-referenced classification or ambiguous fingerprint

Besides, about 9.53% of the fingerprints is of low quality caused by dry, wet, cuts, bruises, and low contrast [13]. Worse still, almost all prints in the NIST Db-14 contain extraneous objects like handwritten annotations and other artefacts common to inked fingerprints. The unavoidable annotation resulted from the labelling process performed by the human experts who are tasked to manually classify the fingerprint (see Fig. 6).

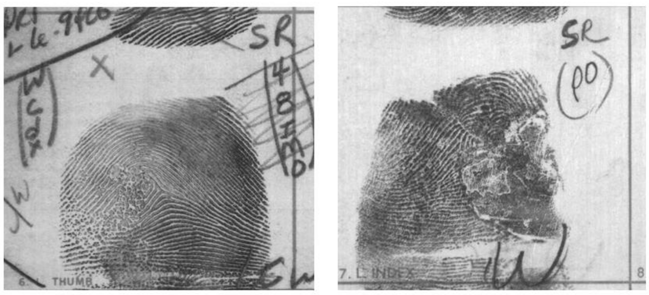

(a) (b)

Fig. 6 Fingerprint with extraneous objects: (a) like handwritten characters and (b) other artefacts common to inked fingerprints

In order to accomplish the task, the performance is measured in terms of error rate or accuracy. The error rate is computed as the ratio between the number of misclassified fingerprints and the total number of samples in the test set. The accuracy is thus the percentage of correctly classified fingerprints [11].

Subsequently, a confusion matrix is created based on the above error rate that provides detailed performance of the proposed classification technique with regards to the experimental results. There are two main components of the matrix, namely true class and hypothesized class. The former represents a certified class provided by the human experts and is labelled in the NIST Db-14, while the latter indicates a computed class produced by the proposed classification method. Figures located in a diagonal stripe represent correctly classified prints, while amounts of the diagonal stripe indicate misclassifications. The correctly classified means that the hypothesized class is matched with the actual class extracted from the NIST Db-14. Otherwise, it is considered as misclassified print.

Table II shows a confusion matrix of the experimental results of the proposed method. There are 62 rejected or unknown prints of total 27,000 fingerprints. The distribution of the correctly classified prints for Whorl, Left-loop, Right-loop, Arch and Tented-arch classes are 7,189; 7,709; 7,262; 834; and 151, respectively. Distribution of misclassified prints (minus rejected prints) are 1,136; 896; 961; 137; and 663 of the Whorl, Left-loop, Right-loop, Arch and Tented-arch classes, respectively (see Table III).

The experimental results have revealed that the proposed classification technique has precisely classified exactly 85.92%. The percentage is derived from the ratio of 23,145 correctly classified prints and 26,938 total fingerprints (i.e. 27,000 minus 62 of unknown prints that include good, wet, dry, cuts, bruises, low contrast and stains prints (i.e. Fig. 7(a)-(g)). The remaining 14.08% is considered misclassified, which are mainly due to small-interclass variation (i.e. Fig. 9) and poor quality fingerprints (i.e. Fig. 10).

TABLE II
A CONFUSION MATRIX OF THE EXPERIMENTAL RESULTS OF THE PROPOSED FINGERPRINT CLASSIFICATION

True class	Hypothesized class					
	W	L	R	A	T	U
W	**7,189**	582	522	23	9	7
L	544	**7,709**	116	158	78	24
R	502	113	**7,262**	183	163	20
A	13	73	44	**834**	7	10
T	34	222	130	277	**151**	1

W= whorl, L= left-loop, R= right-loop, A= arch, T= tented-arch, U= unknown.

Table II above has also revealed that the accuracy rate for Whorl, Left-loop, Right-loop, Arch and Tented-arch classes are 86.35%, 89.59%, 88.31%, 85.89%, and 18.55%, respectively. The figures show very encouraging results except for Tented-arch. Such low percentage obtained in the Tented-arch case was mainly due ambiguous prints, in which their exclusive class was unclear (see Table III and Fig. 9(a) –(c)).

TABLE III
AMBIGUOUS FINGERPRINTS OF THE MISCLASSIFIED PRINTS

Class	Misclassified	Ambiguous
Whorl	1,136	129
Left-loop	896	123
Right-loop	961	155
Arch	137	7
Tented-arch	663	500

Meanwhile, for the misclassified fingerprints, Tented-arch is the highest in terms of ambiguous prints (see Table III). The Whorl, Left-loop and Right-loop are distant second. shows the ambiguous fingerprints of the misclassified prints in which Tented-arch There are 1.55% represented by 129 ratio ambiguous prints and 8,325 classified prints for Whorl. Next, the distribution of ambiguous fingerprint for Left-loop, Right-loop, Arch and Tented-arch classes are 1.43%, 1.88%, 0.72%, 61.43%, respectively. The remaining is due to the small-interclass variation and poor prints. With regard to the Tented-arch, in actual fact, it is obvious that higher error rate is mainly contributed by ambiguous prints (i.e. 61.43%). Detailed results of the small-interclass variation will be separately discussed in the later part.

TABLE IV
THE ACCURACY RATES OF THE CAPPELLI AND MALTONI'S CLASSIFICATION METHODS [12] AND PROPOSED METHOD

Classification method	Accuracy (%)
Rule based	77.10
Model: Single Gaussian	79.60
Model: Mixture of Gaussian	81.20
Proposed method	89.31

Since most of the ambiguous prints have been assigned with double classes by the fingerprint expert, their exclusive class can be chosen from one of them. Therefore, should rule of thumb was applied and the hypothesized class of misclassified ambiguous prints was accepted as a true class; the overall error rate would be significantly reduced by 3.39%. As a result, the overall accuracy rate would rise to 89.31%. Consequently, new distribution of the improved accuracy rates would be 87.90%, 91.02%, 90.20%, 86.61%, and 79.98% for Whorl, Left-loop, Right-loop, Arch, and Tented-arch, respectively. The results have also proved that the proposed method markedly outperformed the Cappelli and Maltoni's techniques (see Table IV).

Furthermore, in fact, for some prints, especially wet and bruises ones (e.g. Fig. 7 (c) and (e)), which are considered extremely difficult to be classified even by human experts because cores or deltas are missing, have also been precisely classified.

The following discussions are devoted for special prints of both large-intra-class and small-interclass variations. These prints deserve due attentions since their characteristics are considered to be unique.

Overall, the proposed classification technique has successfully classified most of the whorl fingerprints of the intra-class variation (e.g. Fig. 8(a) - (c)). In fact, by closely examined these figures; structure shape of these prints are greatly distinct, for instance Fig. 8(b) and Fig. 8(c) whose shapes are considered abnormal, i.e. contain double loops. Despite of this abnormality, these prints are actually sharing a common feature, which is a set of duo-core and duo-delta. In actual fact, the success was attributed to the strength of the proposed singular point detection approach, which is able to detect the genuine cores and deltas by exploiting true gradients of the orientation fields, which are perfectly matched with close curve nature of the Poincare index.

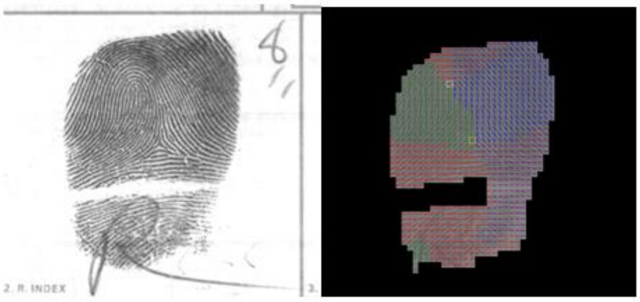

(a) Good fingerprint (file name: f0000002)

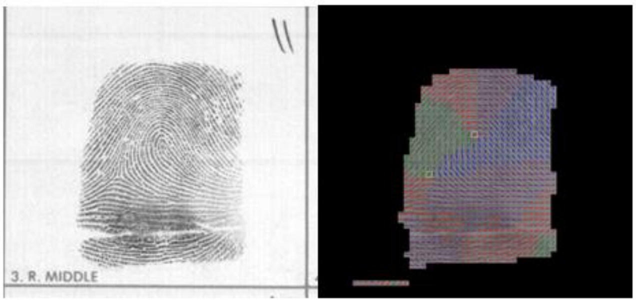

(b) Dry fingerprint (file name: f0000243)

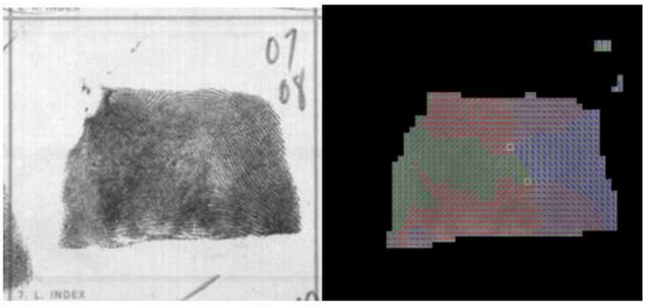

(c) Wet fingerprint (file name: f0000127)

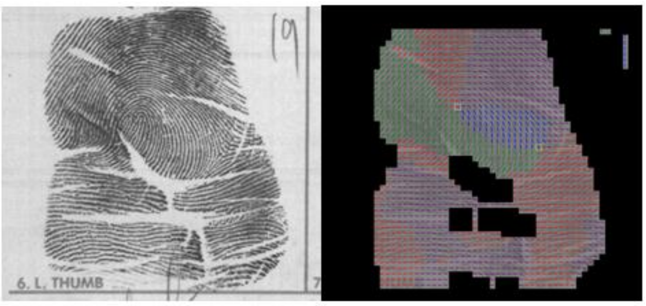

(d) Cut fingerprint (file name: f0010166)

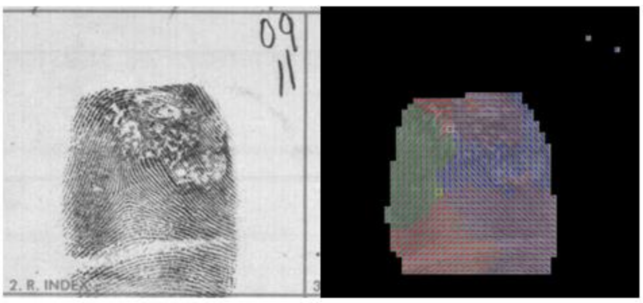

(e) Bruise fingerprint (file name: f00001872)

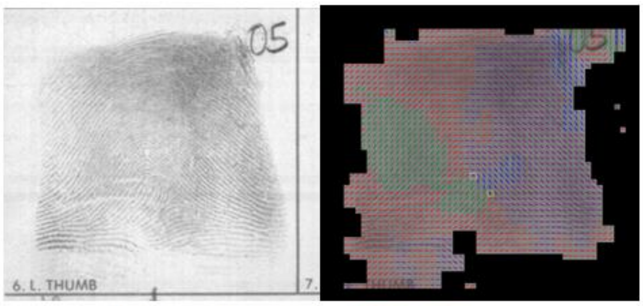

(f) Low contrast fingerprint (file name: f0010206)

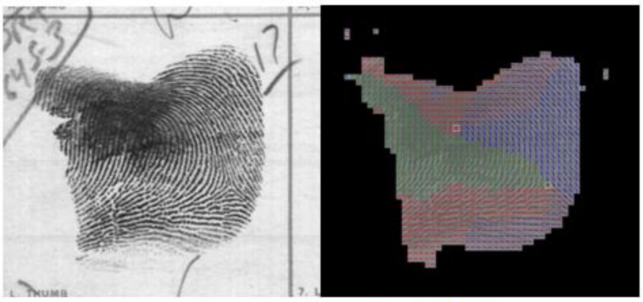

(g) Stain fingerprint (file name: f0010366)

Fig. 7 (a) – (g) Some examples of correctly classified prints of various qualities viz. good, dry, wet, cut, bruise, low contrast, and stain

Contrary to the above case, as for the small-interclass variation (e.g. Fig. 9(a) - (c)); almost all of the Tented-arch prints are failed to be classified correctly. In fact, detailed observation of these prints has revealed that, in most cases, their ridges' structure traverses gradually from left to right without forming a summit (i.e. it rises progressively from the left to the middle and then descends gradually to the right, or vice versa). Consequently, core and delta are nonexistent (Fig. 9(a)). As a result, the Tented-arch is then classified as an Arch class, instead.

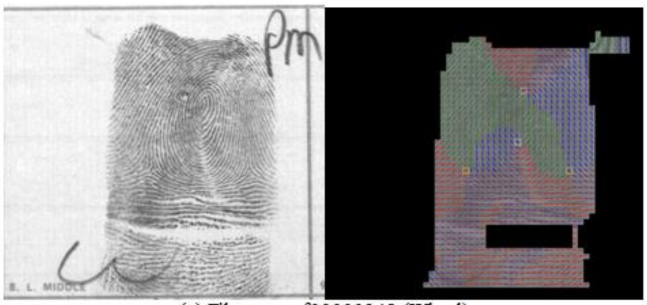

(a) File name: f00000348 (Whorl)

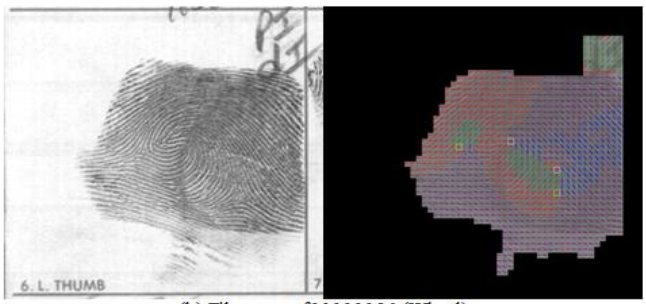

(b) File name: f00000056 (Whorl)

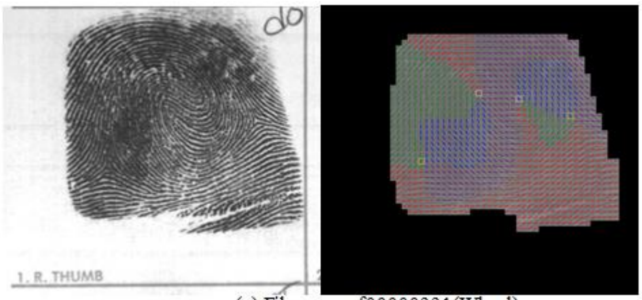

(c) File name: f00000331(Whorl)

Fig. 8 (a) – (c) A sample of large-intra-class variation prints

Meanwhile, for Tented-arch prints which have sufficient peak's height are sometimes closely resemblance to Left-loop or Right-loop because the location of core relative to delta is not in perpendicular position: If the position between them is inclined to the left, then it is classified as a Left-loop (see Fig. 9(b)); otherwise it is a Right-loop class (see Fig. 9(c)). Therefore, as a result, some researchers tend to combine Arch and Tented-arch as one category named Arch class.

Yet another interesting case which has never been discussed in the previous studies of automatic fingerprint classification systems, in which a Whorl print is misclassified as either Right-loop or Left-loop, is discovered in this study (see Fig. 9(d) and (e)). This special type of print is quite common and existed in a significant number in Db-14 (i.e. more than 2000 prints), and therefore should be given due attention. Generally, this particular type of print carries a unique feature in which the gap that separates between lower core and delta is extremely small and almost touching each other. Consequently, both lower core and delta are failed to be detected, and lead to misclassification of Whorl, and thus is mistakenly classified as Right-loop or Left-loop, instead. With regard to this, a new fingerprint class called "Whorl Loop" which is neither Whorl nor Loop is therefore suggested, and an in-depth study is required to reaffirm the finding.

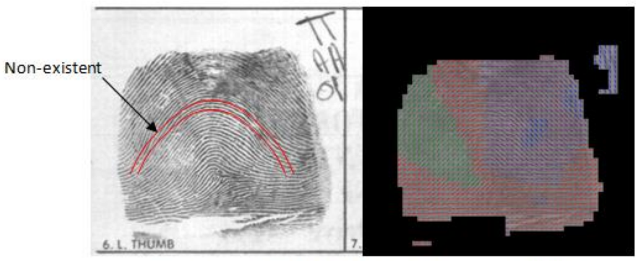

(a) Tented-arch: misclassified as Arch (file name: f0000446)

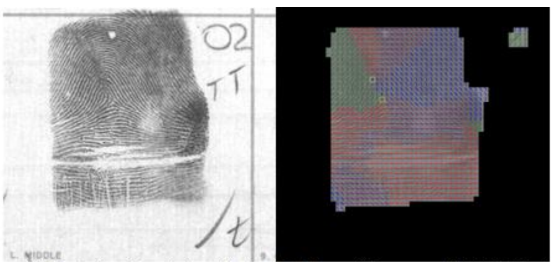

(b) Tented-arch: misclassified as Left-loop (file name: f0000578)

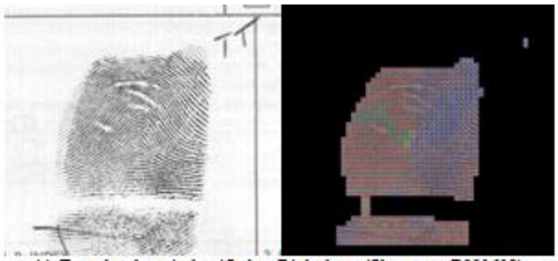

(c) Tented-arch: misclassified as Right-loop (file name: f0001612)

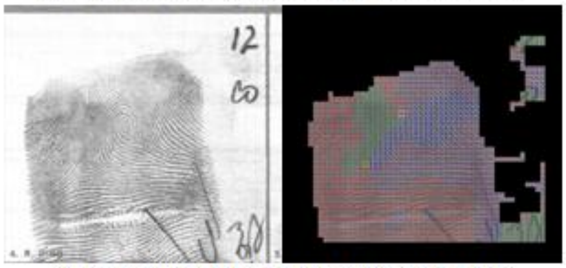

(d) Whorl: misclassified as Right-loop (file name: f0000094)

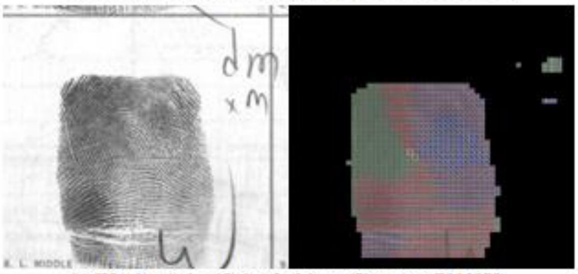

(e) Whorl: misclassified as Left-loop (file name: f0000078)

Fig. 9 (a) – (e) Small inter-class variations

As for the poor quality fingerprint, for instance Fig. 10 has shown that the ridges' structure is badly damaged, and thus created a lot of false deltas and cores. Worse still, the important area of the print becomes background, and as a result some singular points may be disappearing. Therefore, this type of prints is normally rejected rather than carried on with a wrong decision.

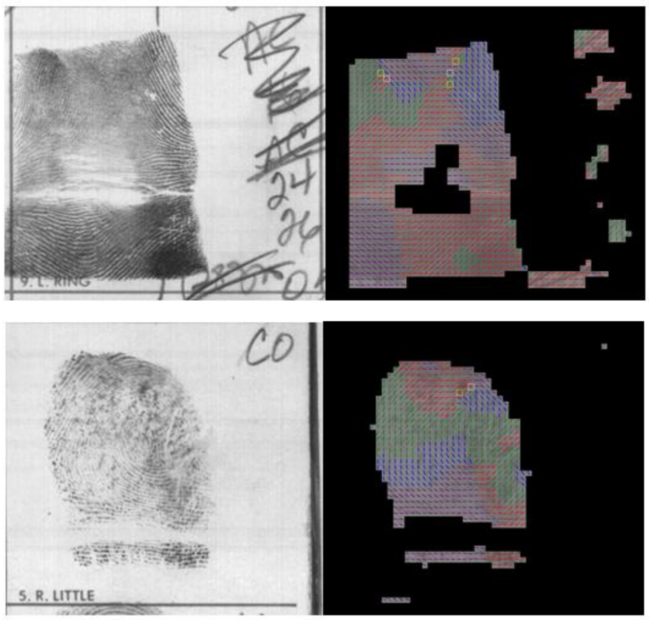

Fig. 10 Poor quality fingerprints

V. Conclusion

In this paper, a new method for automatic fingerprint classification based on singular points and structural shape of orientation fields is proposed. The main contributions of this paper are: (i) a new scheme of fingerprint classification and (ii) an algorithm for automatic classification using rule based on of number and position of singular points that is combined with the structural shape of orientation fields. The algorithm has been tested on 27,000 fingerprint image from NIST Db-14. Experimental results show that our algorithm has a better performance in accuracy for automatic fingerprint classification than the previous works.

Acknowledgment

This research was partially supported by Faculty of Computer Science, Universitas Sriwijaya. We would also appreciate our colleagues' expertise that enormously helped the research.

References

[1] K. Karu and A.K. Jain, "Fingerprint Classification," *Pattern Recognition*, vol. 29, no. 3, pp. 389-404, 1996.

[2] R. Cappelli, A. Lumini, D. Maio, and D. Maltoni, "Fingerprint Classification by Directional Image Partitioning," *IEEE Transactions on Pattern Analysis and Machine Intelligence*, vol. 21, no. 5, pp. 402-421, 1999.

[3] C. Wilson, G. Candela, and C. Watson, "Neural Network Fingerprint Classification," *Journal Art Neural Network*, vol. 1, no. 2, pp. 203–228, 1993.

[4] Saparudin. *An Automatic Fingerprint classification Technique Based on Singular Points and Sructure Shape of Orientation Fields*. Thesis in Computer Science, Universiti Teknologi Malaysia, Johor Baru. 241.

[5] L. Hong and A.K. Jain, "Classification of Fingerprint Images," *11th Scandinavian Conference on Image Analysis, June 7-11,* Kangerlussuaq, Greenland, 1999.

[6] A.K. Jain and S. Minut, "Hierarchical Kernel Fitting for Fingerprint Classification and Alignment," *Proc. Int. Conf. on Pattern Recognition (*16th*)*, 2002.

[7] Q. Zhang and H. Yan, "Fingerprint Classification Based on Extraction and Analysis of Singularities and Pseudo ridges," *Pattern Recognition*, vol. 37, no. 11, pp. 2233-2243, 2004.

[8] X. Wang and M. Xie, "Fingerprint Classification: An Approach Based on Singularities and Analysis of Fingerprint Structure," *Proc. International Conference on Biometric Authentication (1st)*, LNCS 3072. pp. 324-329, 2004.

[9] L. Wang and M. Dai, "Application of a new type of singular points in fingerprint classification. *Pattern Recognition Letters,* vol. 28, no. 13, pp. 1640-1650, 2007.

[10] V. Sasikala and V. Lakshmi Prabha, "Bee Swarm based Feature Selection for Fake and Real Fingerprint Classification using Neural Network Classifiers," *IAENG International Journal of Computer Science*, vol. 42, no. 4, pp. 389-403, 2015.

[11] D. Maltoni, D. Maio, A.K. Jain, and S. Prabhakar, *Handbook of Fingerprint Recognition*. Second edition. Springer-Verlag London Limited, 2009.

[12] C.I. Watson, NIST Special Database 14 Mated Fingerprint Cards Pairs 2 version 2. U.S. National Institute of Standards and Technology, 1993.

[13] R. Cappelli and D. Maltoni, "On the Spatial Distribution of Fingerprint Singularities, "*IEEE Transactions on Pattern Analysis and Machine Intelligence*, vol. 31, no. 4, 2009.

[14] J. Li, W.Y. Yau, and H. Wang, "Combining Singular Points and Orientation Image Information for Fingerprint Classification," *Pattern Recognition*, vol. 41, no. 1, pp. 353-366, 2007.

[15] A.K. Jain, S. Prabhakar, and L. Hong, "A Multichannel Approach to Fingerprint Classification," *Pattern Recognition,* vol. 21, no. 4, pp. 348–359, 1999.

[16] E. Zhu, J. Yin, C. Hu, and G. Zhang, "A Systematic Method for Fingerprint Ridge Orientation Estimation and Image Segmentation," *Pattern Recognition,* vol. 39, pp. 1452-1472, 2006.

[17] C.H. Park, J.J. Lee, M.J.T. Smith, and K.H. Park, "Singular Point Detection by Shape Analysis of Directional Fields in Fingerprints," *Pattern Recognition*, vol. 39, no. 5, pp. 839–855, 2006.

[18] E. Henry, *Classification and Uses of Finger Prints*, George Routledge and Sons, 1990.

[19] M. Chong, T. Ngee, L. Jun, and R. Gay, "Geometric Framework for Fingerprint Image Classification," *Pattern Recognition*, vol. 30, no. 9, pp. 1475–1488, 1997.

[20] B.H. Cho, J.S. Kim, J.H. Bae, I.G. Bae, and K.Y. Yoo, "Core-Based Fingerprint Image Classification," *Proc. Int. Conf. on Pattern Recognition* (15th), vol. 2, pp. 863-866, 2000.

[21] J. Li, W.Y. Yau, and H. Wang, "Constrained Non Linear Models of Fingerprint Orientations with Prediction," *Pattern Recognition*, vol. 39, no. 1, pp. 102-114, 2006.

[22] T. Tan, Y. Zhan, L. Ding, and S. Sheng, "Fingerprint Classification Based on Analysis of Singularities and Geometric Framework," *APPT 2007 Springer-Verlag Berlin Heidelberg, LNCS 4847*, pp. 703-712, 2007.

[23] G.T. Candela, P.J. Grother, C.I. Watson, R.A. Wilkinson, and C.L. Wilson, *PCASYS-A Pattern-level Classification Automation System for Fingerprints*. NIST Technical Report NISTIR 5647, 1995.

[24] N.K. Ratha, S. Chen, and A.K. Jain, "Adaptive Flow Orientation Based Feature Extraction in Fingerprint Images," *Pattern Recognition*, vol. 28, no. 11, pp. 1657-1672, 1995.

[25] A.M. Bazen and S.H. Gerez, "Systematic Methods for the Computation of the Directional Fields and Singular Points of Fingerprints," *IEEE Transactions on Pattern Analysis and Machine Intelligence*, vol. 24, no. 7, pp. 905-919, 2002.

[26] V. Conti, C. Militello, F. Sorbello, and S. Vitabile, "Introducing Pseudo-Singularity Points for Efficient Fingerprints Classification and Recognition," *IEEE Proc. Int. Conf. on Complex, Intelligent and Software Intensive Systems,* pp. 368-375, 2010.

[27] D. Maio and D. Maltoni, "A Structural Approach to Fingerprint Classification," *Proc. Int. Conf. on Pattern Recognition (13th)*, pp. 578-585, 1996.

[28] R. Cappelli, D. Maio, and D. Maltoni, "Multi-Classifier Approach to Fingerprint Classification," *Pattern Analysis and Application*, vol. 5, pp. 136-144, 2002.

[29] M. Neuhaus and H. Bunke, "A Graph Matching Based Approach to Fingerprint Classification Using Directional Variance," *Proc. Int. Conf. on Audio and Video Based Biometric Person Authentication (5th)*, pp. 191-200, 2005.

[30] V. Conti, G. Pilato, S. Vitabile, and F. Sorbello, "Verification of Ink-on-paper Fingerprints by Using Image Processing Techniques and a New Matching Operator," Proc. of VIII Convegno AI*IA. 2002.

Saparudin was born in Pangkalpinang, Indonesia, in 1969. He received the bachelor degree in Mathematic Education from Universitas Sriwijaya, Indonesia in 1993, and master degree in Informatics Engineering from Institut Teknologi Bandung, Indonesia, in 2000 and Ph.D. degree in Computer Science from Universiti Teknologi Malaysia in 2012.
In 1995, he joined the Department of Informatics, Faculty of Computer Science, Universitas Sriwijaya as an Associate Professor. His current research interest includes; image processing, computer vision, and pattern recognition.

Ghazali Sulong is a Professor in Image processing, Faculty of Computing, Universiti Technologi Malaysia. He received the B.Sc. in Statistics from Universiti Kebangsaan Malaysia in 1979, The M.Sc. and Ph.D. degrees in Computing from University of Wales, College of Cardiff, Wales, United Kingdom, in 1982 and 1989, respectively. His current research interest includes; image processing, computer vision, pattern recognition, and multimedia.